

## Supplementary Information

### Superpotential enhanced superconductivity and robust stiffness shaped by quantum geometry

## I. MODEL AND ELECTRONIC STRUCTURE

Our investigations are based on the attractive Hubbard model

$$H = -t \sum_{\langle ij \rangle, \sigma} c_{i,\sigma}^\dagger c_{j,\sigma} + \sum_{i\sigma} (V_i - \mu) n_{i\sigma} - |U| \sum_n [n_{n,\uparrow} - \langle n_{n,\uparrow} \rangle] [n_{n,\downarrow} - \langle n_{n,\downarrow} \rangle] \quad (1)$$

with on-site interaction  $-|U|$  between charge fluctuations and we restrict to hopping between nearest neighbor sites  $\mathbf{R}_i$ ,  $\mathbf{R}_j$  indicated by  $\langle ij \rangle$ . For the local potential  $V_i$  we consider a checkerboard geometry with alternating  $4 \times 4$  plaquettes within which  $V_i$  alternates between the values  $V_i = 0$  and  $V_i = -V_0$ .

The primitive vectors of the superlattice are  $\vec{r}_1 = (8a, 0)$  and  $\vec{r}_2 = (4a, 4a)$  which gives rise to the reduced Brillouin zone indicated in Fig. 1. The reciprocal lattice is generated by the vectors  $\vec{b}_1 = \frac{\pi}{4a}(1, -1)$  and  $\vec{b}_2 = \frac{\pi}{2a}(0, 1)$ . In the following we set the lattice constant to  $a = 1$ . Upon mean-field decoupling the Fourier transformed hamiltonian Eq. (1) reads

$$H = \sum_{k,n} ' (\varepsilon_{k+Q_n} - \mu) \left[ c_{k,\uparrow}^\dagger(n) c_{k,\uparrow}(n) + c_{-k,\downarrow}^\dagger(n) c_{-k,\downarrow}(n) \right] + \sum_{k,n,m} ' \left[ V_{Q_m} c_{k,\uparrow}^\dagger(n+m) c_{k,\uparrow}(n) + h.c. \right] + \sum_{k,n,m} ' \left[ \Delta_{Q_m} c_{k,\uparrow}^\dagger(n+m) c_{-k,\downarrow}^\dagger(n) + h.c. \right] \quad (2)$$

where the primed sum runs over  $k$ -points of the reduced BZ,  $c_{k,\uparrow}(n) \equiv c_{k+Q_n,\uparrow}$ ,  $c_{-k,\downarrow}(n) \equiv c_{-k-Q_n,\downarrow}$  and  $Q_n$  refers to the reciprocal lattice vectors generated by  $\vec{b}_{1,2}$ . The Fourier transformed potential is  $V_{Q_m} = \frac{1}{N} \sum_n V_n e^{i Q_m R_n}$  and similarly the order parameter is defined as  $\Delta_{Q_m} = \frac{1}{N} \sum_n \Delta_n e^{i Q_m R_n}$  with  $\Delta_n = -|U| \langle c_{n,\downarrow} c_{n,\uparrow} \rangle$ .

In the normal state ( $\Delta_{Q_m} = 0$ ) the hamiltonian Eq. (2) can be diagonalized via

$$c_{k,\uparrow}(n) = \sum_p \Phi_{k,n,\uparrow}(p) a_{k,p,\uparrow} \quad (3)$$

$$c_{-k,\downarrow}(n) = \sum_p \Phi_{-k,n,\downarrow}(p) a_{-k,p,\downarrow} \quad (4)$$

where the index  $p$  refers to the band with energy  $E_{p,\sigma}(k)$ .

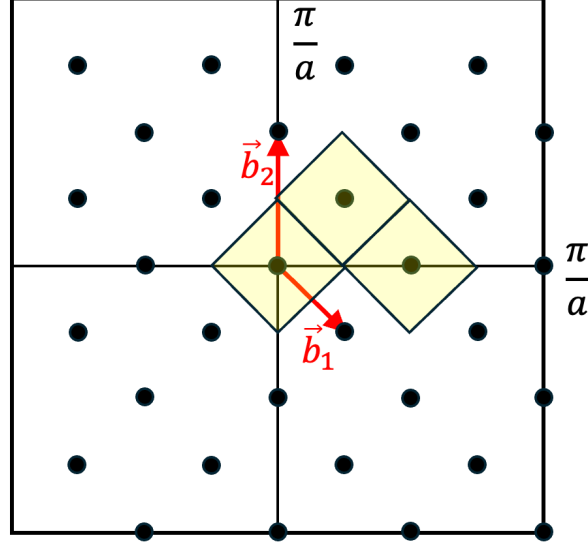


FIG. 1. Reduced Brillouin zone and reciprocal lattice vectors for the considered superpotential consisting of  $4 \times 4$  plaquettes.

In the basis states defined via Eqs. (3,4) the hamiltonian reads

$$H = \sum'_{k,p} \left[ E_{p,\uparrow}(k) a_{k,p,\uparrow}^\dagger a_{k,p,\uparrow} - E_{p,\downarrow}(-k) a_{-k,p,\downarrow}^\dagger a_{-k,p,\downarrow} \right] + \sum'_{k,p,p'} \left[ B_k^*(p',p) a_{k,p,\uparrow}^\dagger a_{-k,p,\downarrow}^\dagger + h.c. \right] \quad (5)$$

with  $B_k^*(p',p) = \sum_{n,m} \Delta_{Q_n} \Phi_{k,n+m,\uparrow}^*(p) \Phi_{-k,m,\downarrow}^*(p')$ . It can be diagonalized via  $H_{diag} = \hat{T}^{-1} \hat{H} \hat{T}$  where the diagonalized hamiltonian has the structure

$$\{H_{diag}\} = \begin{pmatrix} -\Omega_{p<} & 0 \\ 0 & \Omega_{p>} \end{pmatrix} \quad (6)$$

where the index  $p_{<(>)}$  refers to the set of negative (positive) energies. The order parameter can be self-consistently calculated from

$$\begin{aligned} \Delta_{Q_n}^* &= -|U| \langle c_{-k,\downarrow}(n+m) c_{k,\uparrow}(m) \rangle \\ &= -|U| \sum'_{\substack{k,m,j,j' \\ p<,p>}} \Phi_{-k,n+m,\downarrow}(j) \Phi_{k,m,\uparrow}(j') \\ &\quad \times [T_{N+j,p<}^* T_{N+j',p<} (1 - f(\Omega_{p<})) \\ &\quad + T_{N+j,p>}^* T_{N+j',p>} f(\Omega_{p>})] \end{aligned} \quad (7)$$

and  $f(\omega)$  denotes the Fermi distribution. A similar expression can be derived for the charge density which is then used to self-consistently adjust the chemical potential.

## II. CONSIDERATION OF IMPURITIES: REAL SPACE APPROACH

The hamiltonian Eq. (1) is supplemented with an impurity potential  $V = \sum_{n\sigma} I_n n_{n\sigma}$  where the  $I_n$  are drawn from a flat distribution with  $-I_0 \leq I_n \leq I_0$ .

The resulting hamiltonian is then solved on finite lattices in mean-field using the Bogoljubov-de Gennes (BdG) transformation

$$c_{i\sigma} = \sum_k \left[ u_i(k) \gamma_{k,\sigma} - \sigma v_i^*(k) \gamma_{k,-\sigma}^\dagger \right]$$

which yields the eigenvalue equations

$$\begin{aligned} \omega_k u_n(k) &= \sum_j t_{nj} u_j(k) + [I_n + V_n - \mu] u_n(k) \\ &\quad + \Delta_n v_n(k) \end{aligned} \quad (8)$$

$$\begin{aligned} \omega_k v_n(k) &= - \sum_j t_{nj} v_j(k) - [I_n + V_n - \mu] u_n(k) \\ &\quad + \Delta_n^* u_n(k), \end{aligned} \quad (9)$$

where again the  $V_n$  refer to the superpotential at site  $R_n$ .

From the eigenvalue problem Eqs. (8,9) one can iteratively determine the BdG amplitudes  $u_i(k), v_i(k)$  which allow for the self-consistent evaluation of local densities and order parameters.

## III. CURRENT CORRELATIONS

The evaluation of the superfluid stiffness in the main paper is based on the current-current correlation function

$$\chi_{nm}^{\alpha\beta}(\hat{j}_n^\alpha, \hat{j}_m^\beta) = -i \int dt e^{i\omega t} \langle \mathcal{T} \hat{j}_n^\alpha(t) \hat{j}_m^\beta(0) \rangle \quad (10)$$

where  $\hat{j}_n^\alpha$  corresponds to the paramagnetic current operator on the link  $\mathbf{R}_n$ ,  $\mathbf{R}_n + \mathbf{e}_\alpha$  with  $\alpha = x, y$ , i.e.

$$\hat{j}_n^\alpha = it \sum_\sigma \left[ c_{n+\alpha,\sigma}^\dagger c_{n,\sigma} - c_{n,\sigma}^\dagger c_{n+\alpha,\sigma} \right]. \quad (11)$$

Using the transformations from the previous subsection the current-current correlation function can be represented in the following form

$$\begin{aligned} \chi^{\alpha\beta}(\omega) &= \frac{1}{N} \sum'_{\substack{k,r,t,n,m \\ p_<,p_>}} C_{r,t}^\alpha(k, p_<, p_>) C_{m,n}^{\beta,*}(k, p_<, p_>) \\ &\quad \times \left[ \frac{1}{\omega - \Omega_{p_>} - \Omega_{p_<} - i\eta} - \frac{1}{\omega + \Omega_{p_>} + \Omega_{p_<} - i\eta} \right] \end{aligned} \quad (12)$$

where the matrix elements of the current operator are given by

$$\begin{aligned} C_{r,t}^\alpha(k, p_<, p_>) &= -2t \sum_n \sin(k_\alpha + Q_n^\alpha) \\ &\times [\Phi_{k,n,\uparrow}^*(r) \Phi_{k,n,\uparrow}(t) T_{r,p_<}^* T_{t,p_>} \\ &+ \Phi_{-k,n,\downarrow}^*(r) \Phi_{-k,n,\downarrow}(t) T_{N+t,p_<}^* T_{N+r,p_>}] . \end{aligned} \quad (13)$$

The expression for the stiffness given in Eq. (3) of the main paper includes the kinetic energy in direction  $\alpha$  which is given by

$$\langle t_\alpha \rangle \equiv \frac{1}{N} \sum_{\substack{k,s,t \\ p_<,p_>}} \tau_{s,t}^\alpha(k, p_<, p_>) \quad (14)$$

$$\begin{aligned} \tau_{s,t}^\alpha(k, p_<, p_>) &= -2t \sum_n' \cos(k_\alpha + Q_n^\alpha) \\ &\times [\Phi_{k,n,\uparrow}^*(s) \Phi_{k,n,\uparrow}(t) T_{s,p_<}^* T_{t,p_<} \\ &+ \Phi_{-k,n,\downarrow}^*(s) \Phi_{-k,n,\downarrow}(t) T_{N+t,p_>}^* T_{N+s,p_>}] . \end{aligned} \quad (15)$$

#### IV. INCLUSION OF FLUCTUATIONS IN THE EVALUATION OF THE CURRENT CORRELATION FUNCTION

For larger values of the interaction  $|U|/t \gtrsim 1$  phase relaxation processes increasingly renormalize the stiffness. These can be included by dressing the current-current correlations with pair and charge fluctuations

$$\begin{aligned} \delta\Delta_i &\equiv c_{i\downarrow} c_{i\uparrow} - \langle c_{i\downarrow} c_{i\uparrow} \rangle_0 \\ \delta n_i^\dagger &\equiv \sum_\sigma \left( c_{i\sigma}^\dagger c_{i\sigma} - \langle c_{i\sigma}^\dagger c_{i\sigma} \rangle_0 \right) \\ \delta\Delta_i^\dagger &\equiv c_{i\uparrow}^\dagger c_{i\downarrow} - \langle c_{i\uparrow}^\dagger c_{i\downarrow} \rangle_0 \end{aligned}$$

for which the corresponding correlation functions can be defined similar to Eq. (10). Here and in the following a nought sub- or superscript denotes evaluation in the BdG ground state.

Defining also the matrix of local interactions  $\underline{\underline{V}}$  between pair and charge fluctuations the resummation

$$\underline{\underline{\chi}} = \left[ \underline{\underline{1}} - \underline{\underline{\chi}}^0 \underline{\underline{V}} \right]^{-1} \underline{\underline{\chi}}^0 \quad (16)$$

allows to compute the dynamical amplitude  $A_i \equiv (\delta\Delta_i + \delta\Delta_i^\dagger)/\sqrt{2}$  and phase  $\Phi_i \equiv (\delta\Delta_i - \delta\Delta_i^\dagger)/\sqrt{2}$  correlations.

Vertex corrections to the bare current-current correlation function  $\chi_{nm}^0(j_n^\alpha, j_m^\beta)$  can be obtained by defining  $\Lambda_{nm}^\alpha = \chi^0(j_n^\alpha, \hat{A}_m)$  and  $\bar{\Lambda}_{nm}^\alpha = \chi^0(\hat{A}_n, j_m^\alpha)$  which couple the current  $j_m^\alpha$  between sites  $R_m$  and  $R_{m+\alpha}$  to the pair and charge fluctuations. The full (gauge invariant) current correlation function is then obtained from

$$\begin{aligned}
\chi_{nm}(j_n^\alpha, j_m^\beta) &= \chi_{nm}^0(j_n^\alpha, j_m^\beta) + \Lambda_{nm}^\alpha V_{mk} \bar{\Lambda}_{km}^\beta \\
&\quad + \Lambda_{nm}^\alpha V_{mk} \chi_{kl} V_{ls} \bar{\Lambda}_{sm}^\beta \\
&= \chi_{nm}^0(j_n^\alpha, j_m^\beta) \\
&\quad + \Lambda_{nm}^\alpha V_{mk} \left[ \frac{1}{\omega - \Omega_{p<} - \Omega_{p>} + i\eta} \right]_{kl}^{-1} \bar{\Lambda}_{lm}^\beta \\
&\equiv \chi_{nm}^{BCS}(j_n^\alpha, j_m^\beta) + \chi_{nm}^{RPA}(j_n^\alpha, j_m^\beta). \tag{17}
\end{aligned}$$

In momentum space the correlation functions for the vertices are explicitly given by

$$\begin{aligned}
\chi^0(j(0), \delta\Delta_{-Q_n}^\dagger) &= \sum_{\substack{k,m,m' \\ s,t,s',t'}} \Phi_{k+Q_{m'-Q_n},\uparrow}^*(s') \Phi_{-k-Q_{m'},\downarrow}^*(t') \\
&\quad \times \left\{ \frac{C_{s,t}^{k,m}(p_<, p_>) T_{s',p_>}^* T_{N+t',p_<}}{\omega - \Omega_{p<} - \Omega_{p>} + i\eta} + \frac{(C_{t,s}^{k,m})^*(p_<, p_>) T_{s',p_<}^* T_{N+t',p_>}}{\omega + \Omega_{p<} + \Omega_{p>} - i\eta} \right\} \\
\chi^0(j(0), \delta\Delta_{Q_n}) &= \sum_{\substack{k,m,m' \\ s,t,s',t'}} \Phi_{-k-Q_{m'}+Q_n,\downarrow}^*(s') \Phi_{k+Q_{m'},\uparrow}^*(t') \\
&\quad \times \left\{ \frac{C_{s,t}^{k,m}(p_<, p_>) T_{N+s',p_>}^* T_{t',p_<}}{\omega - \Omega_{p<} - \Omega_{p>} + i\eta} - \frac{(C_{t,s}^{k,m})^*(p_<, p_>) T_{N+s',p_<}^* T_{t',p_>}}{\omega + \Omega_{p<} + \Omega_{p>} - i\eta} \right\} \\
\chi^0(j(0), \delta\rho_{-Q_n}) &= \sum_{\substack{k,m,m' \\ s,t,s',t'}} \left\{ \frac{C_{s,t}^{k,m}(p_<, p_>) R_{2,s',t'}^{k,m'}(p_<, p_>)}{\omega - \Omega_{p<} - \Omega_{p>} + i\eta} - \frac{(C_{t,s}^{k,m})^*(p_<, p_>) R_{1,s',t'}^{k,m'}}{\omega + \Omega_{p<} + \Omega_{p>} - i\eta} \right\}
\end{aligned}$$

with

$$\begin{aligned}
R_{1,s',t'}^{k,m'} &= \Phi_{k+Q_{m'-Q_n},\uparrow}^*(s') \Phi_{k+Q_{m'},\uparrow}^*(t') T_{s',p_<}^* T_{t',p_>} - \Phi_{-k-Q_{m'}-Q_n,\downarrow}^*(s') \Phi_{-k-Q_{m'},\downarrow}^*(t') T_{N+s',p_>}^* T_{N+t',p_<}^* \\
R_{2,s',t'}^{k,m'} &= \Phi_{k+Q_{m'-Q_n},\uparrow}^*(s') \Phi_{k+Q_{m'},\uparrow}^*(t') T_{s',p_>}^* T_{t',p_<} - \Phi_{-k-Q_{m'}-Q_n,\downarrow}^*(s') \Phi_{-k-Q_{m'},\downarrow}^*(t') T_{N+s',p_<}^* T_{N+t',p_>}.
\end{aligned}$$

Similarly, the correlation functions between the fluctuations read as

$$\begin{aligned}
\chi^0(\delta\Delta_{Q_n}^\dagger, \delta\Delta_{-Q_{n'}}^\dagger) &= \sum_{k,m,m'} \left\{ \frac{T_{n+m,p<}^* T_{N+m,p>} T_{-n'+m',p>}^* T_{N+m',p<}}{\omega - \Omega_{p<} - \Omega_{p>} + i\eta} - \frac{T_{-n'+m',p<}^* T_{N+m',p>} T_{n+m,p>}^* T_{N+m,p<}}{\omega + \Omega_{p<} + \Omega_{p>} - i\eta} \right\} \\
\chi^0(\delta\Delta_{Q_n}^\dagger, \delta\Delta_{Q_{n'}}) &= \sum_{k,m,m'} \left\{ \frac{T_{n+m,p<}^* T_{N+m,p>} T_{N-n'+m',p>}^* T_{m',p<}}{\omega - \Omega_{p<} - \Omega_{p>} + i\eta} - \frac{T_{N-n'+m',p<}^* T_{m',p>} T_{n+m,p>}^* T_{N+m,p<}}{\omega + \Omega_{p<} + \Omega_{p>} - i\eta} \right\} \\
\chi^0(\delta\Delta_{-Q_n}, \delta\Delta_{Q_{n'}}) &= \sum_{k,m,m'} \left\{ \frac{T_{N+n+m,p<}^* T_{m,p>} T_{N-n'+m',p>}^* T_{m',p<}}{\omega - \Omega_{p<} - \Omega_{p>} + i\eta} - \frac{T_{N-n'+m',p<}^* T_{m',p>} T_{N+n+m,p>}^* T_{m,p<}}{\omega + \Omega_{p<} + \Omega_{p>} - i\eta} \right\} \\
\chi^0(\delta\Delta_{Q_n}^\dagger, \delta\rho_{-Q_{n'}}) &= \sum_{k,m,m'} \left\{ \frac{T_{n+m,p<}^* T_{N+m,p>} (T_{m'-n',p>}^* T_{m',p<} - T_{N+m',p>}^* T_{N+m'+n',p<})}{\omega - \Omega_{p<} - \Omega_{p>} + i\eta} \right. \\
&\quad \left. - \frac{T_{n+m,p>}^* T_{N+m,p<} (T_{m'-n',p<}^* T_{m',p>} - T_{N+m',p<}^* T_{N+m'+n',p>})}{\omega + \Omega_{p<} + \Omega_{p>} - i\eta} \right\} \\
\chi^0(\delta\Delta_{-Q_n}, \delta\rho_{-Q_{n'}}) &= \sum_{k,m,m'} \left\{ \frac{T_{N+n+m,p<}^* T_{m,p>} (T_{m'-n',p>}^* T_{m',p<} - T_{N+m',p>}^* T_{N+m'+n',p<})}{\omega - \Omega_{p<} - \Omega_{p>} + i\eta} \right. \\
&\quad \left. - \frac{T_{N-n+m,p>}^* T_{m,p<} (T_{m'-n',p<}^* T_{m',p>} - T_{N+m',p<}^* T_{N+m'+n',p>})}{\omega + \Omega_{p<} + \Omega_{p>} - i\eta} \right\}
\end{aligned}$$

Inserting these correlation functions into Eq. (17) defines the RPA kernel from Eq. (4) of the main paper.

As discussed in the main text, inclusion of charge and phase fluctuations restores gauge invariance by taking into account phase relaxation processes.

Fig. 2 shows the BCS currents for an applied vector potential along the x-direction and in the presence of the superpotential. This figure should be compared with the corresponding gauge invariant result, shown in Fig. 2 of the main paper. Clearly, the BCS currents don't obey charge conservation which can be most clearly seen at the edges of the SC regions. For example, at sites (4, 6 and (4, 7) the incoming currents are significantly larger than the outgoing ones and therefore violate Kirchhoff's law.

In Fig. 3 we report the interaction dependence of the stiffness, both for BCS and BCS+RPA, for a smaller value  $V_0/t = 2$  of the superpotential than reported in the main paper in Fig. 3. Also in this case one observes an increase of  $D_s$  with increasing  $|U|/t$ , however, the curves extrapolate to a finite charge stiffness at  $|U|/t = 0$ . Moreover, the positive interband term  $D_{r \neq m}^{geom}$  (black curve) now continuously increases with  $|U|/t$  and constitutes a fraction of  $\sim 40\%$  to the total stiffness at  $|U|/t = 3$ .

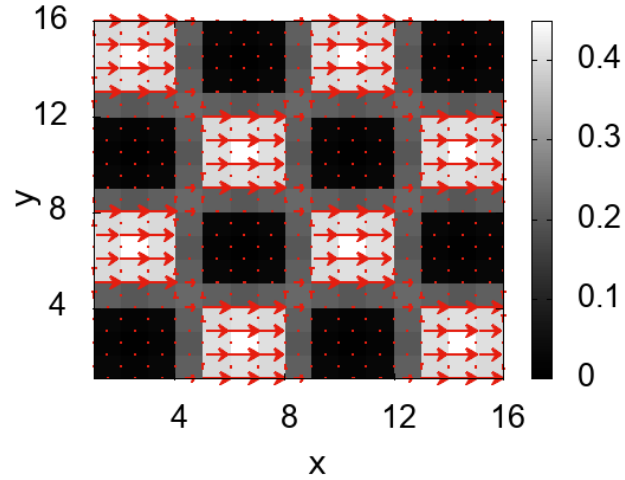


FIG. 2. BCS SC current distribution for a vector potential applied along the x-direction. The local gaps are shown as grey background.  $U/t = 2$ ,  $V_0/t = 4$ , Charge concentration  $n_{el} = 0.5$ .

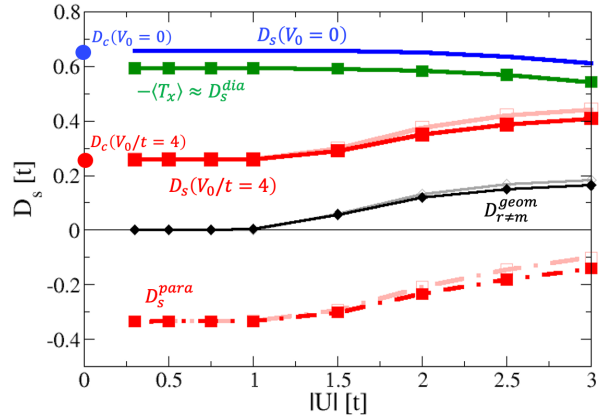


FIG. 3. Interaction dependence of the stiffness  $D_{s,tot}$  for superpotential values  $V_0/t = 0$  (blue) and  $V_0/t = 2$  (red, squares) separated into the diamagnetic (mostly intraband) ( $D_s^{dia}$ ) and paramagnetic (mostly interband) ( $D_s^{para}$ ) contribution. Also shown is the geometric contribution for  $r \neq m$  (black) which positively contributes to the stiffness. Lines in the foreground (full symbols) and in the background (open symbols) refer to the RPA (BCS) result, respectively. For  $|U|/t = 0$  the charge stiffness  $D_c$  is shown by full circles while  $D_s$  vanishes in this limit. charge concentration:  $p = 0.5$ .

## V. DETERMINATION OF $k_F$

In order to estimate the value for the scattering rate in the disordered system, we calculate the normal state optical conductivity without superpotential but disorder potential  $I_0/t = 0.5$  and  $I_0/t = 1.0$  from an average over 10 disorder configurations, cf. Fig. 4. This result is then fitted by a standard Drude form

$$\sigma(\omega) = \frac{\sigma_0}{1 + \omega^2 \tau^2} \quad (18)$$

which for  $I_0/t = 0.5$  yields  $\sigma_0 \approx 11$  and  $\tau = 15[1/t]$ . In case of  $I_0/t = 1.0$  one obtains  $\sigma_0 = 2.5$  and  $\tau \approx 3.8[1/t]$ .

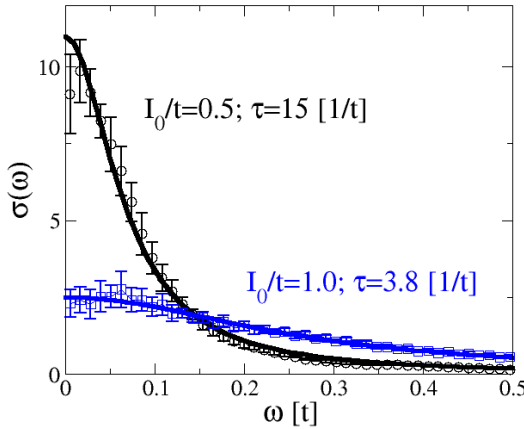


FIG. 4. Drude fit (lines) to the numerical (symbols) normal state optical conductivity without superpotential but disorder  $I_0/t = 0.5$  (black),  $I_0/t = 1.0$  (blue) and density  $n_{el} = 0.5$ . The numerical  $\sigma(\omega)$  is obtained from an average over 10 disorder configurations.

From the bare bandstructure one can average Fermi momentum and Fermi velocity for given chemical potential at  $n_{el} = 0.5$ . This yields  $k_F \approx 1.78[1/a]$  and  $v_F \approx 1.51[ta]$ , so that we obtain for the disorder parameter  $k_Fl = k_Fv_F\tau \approx 40$  in case of  $I_0/t = 0.5$  and  $k_Fl = 10$  for  $I_0/t = 1.0$ .

## VI. SUM RULE AND SPECTRAL WEIGHT TRANSFER

The optical conductivities in normal ( $\sigma_{NL}$ ) and superconducting ( $\sigma_{SC}$ ) system follow from the current correlation function and read

$$\sigma_{NL}(\omega) = \pi D_c \delta(\omega) + \frac{Im\chi^{xx}(\omega)}{\omega} \quad (19)$$

$$\sigma_{SC}(\omega) = \pi D_s \delta(\omega) + \frac{Im\chi^{xx}(\omega)}{\omega} \quad (20)$$

where both obey the f-sum rule

$$\int_0^\infty d\omega \sigma_{NL/SC}(\omega) = -\frac{\pi}{2} \langle t_x^{NL/SC} \rangle. \quad (21)$$

From these relations one can construct the identity

$$D_s = \frac{2}{\pi} \int_{0^+}^\infty d\omega [\sigma_{NL}(\omega) - \sigma_{SC}(\omega)] + \langle t_x^{NL} \rangle - \langle t_x^{SC} \rangle + D_c \quad (22)$$

where the integral excludes the contribution of the  $\delta$ -functions.

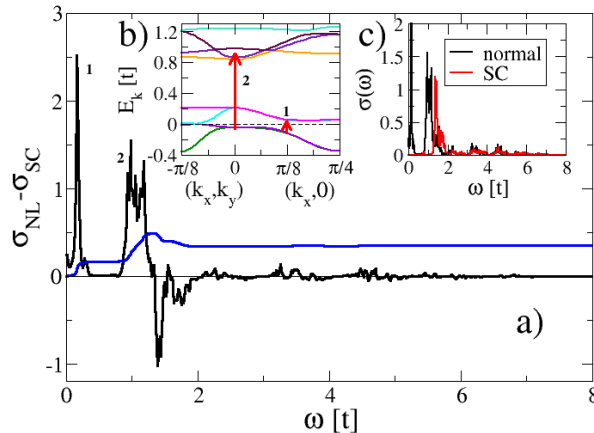


FIG. 5. Main panel: Difference in interband optical spectral weight between normal and superconducting state. The blue solid line corresponds to the integrated spectral weight which determines the interband contribution to  $D_s$ . b) Normal state band structure close to the Fermi energy. Arrows indicate the lowest relevant interband excitations in the main panel. c) Interband optical conductivity for normal and superconducting state. Parameters:  $V_0/t = 4$ ,  $|U|/t = 2$ ,  $n_{el} = 0.5$ .

Fig. 5 reports the spectral weight transfer for a superpotential  $V_0/t = 4$  where the second line of Eq. (22) gives only a minor contribution to the stiffness ( $\langle t_x^{NL} \rangle - \langle t_x^{SC} \rangle + D_c \approx -0.0075$ ) which therefore is essentially determined by the interband spectral weight transfer. The interband optical conductivities in the normal and superconducting state are shown in Fig. 5b. Due to the opening of the gap the optical weight is generally shifted to higher energies in the SC state where the difference to the normal state decreases with increasing energy. As a result the most pronounced difference, which is reported in the main panel, originates from interband excitations up to energies of the order  $\sim t$ . These are indicated in panel b) which shows the low energy band structure for  $V_0/t = 4$  along diagonal and horizontal cuts across the reduced Brillouin zone.

## VII. ORIGIN OF SPECTRAL WEIGHT TRANSFER

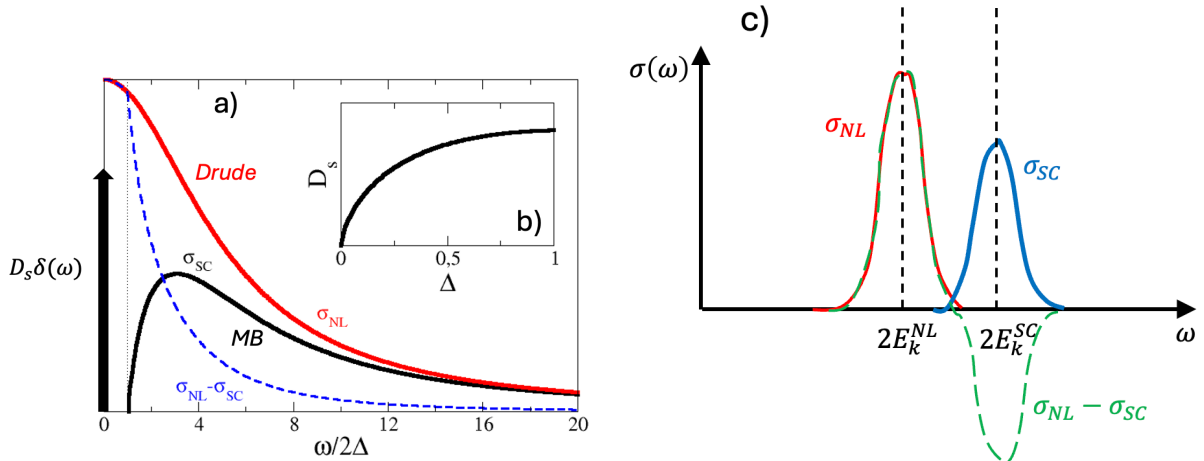


FIG. 6. a) Normal state optical conductivity from Drude theory (red) and in the superconducting state from Mattis-Bardeen theory (black). The area under the difference curve (blue, dashed) yields the superfluid stiffness. b) Dependence of  $D_s$  on the SC gap. c) Optical conductivity for a specific excitation in the presence of a superpotential in the normal (red) and SC state (blue) as explained in the text.

The physics for the optical weight transfer in the presence of a superpotential bears some resemblance with the situation in strongly disordered superconductors. Fig. 6 shows  $\sigma(\omega)$  as obtained from Mattis-Bardeen (MB) theory [1] at zero temperature. Absorption in the SC starts above the energy of the spectral gap  $2\Delta$  and approaches the normal state conductivity

(red) for large energies. For weak coupling the difference of kinetic energies between SC and normal state can be neglected and for a Drude -like normal conductivity  $D_c = 0$  in the sum rule Eq. (22). Therefore, the superfluid stiffness is determined from the integrated difference  $\sigma_{NL}(\omega) - \sigma_{SC}(\omega)$  which naturally scales with the spectral gap  $2\Delta$ , cf. Fig. 6b. Since  $\Delta$  increases with the interaction this is similar to what is observed in Fig. 3 in the main paper in the presence of a superpotential. In fact, in MB theory absorption is induced by the violation of momentum conservation due to the scattering from impurities while here the scattering from the superpotential causes the paramagnetic absorption processes. The spectral weight transfer can be understood from the modification of the band structure due to the scattering from the superpotential and the SC gap. Consider two states close to the Fermi surface which can be connected by one of the reciprocal lattice vectors  $Q_n$ . The resulting new states have energies  $E_k^{NL} = \pm\sqrt{(\varepsilon_k - \mu)^2 + V_{Q_n}^2}$  which leads to a peak in the optical conductivity at  $\omega = 2E_k^{NL}$  (assuming that  $\mu$  stays approximately the same). In the presence of SC the energies are modified to  $E_k^{NL} = \pm\sqrt{(\varepsilon_k - \mu)^2 + V_{Q_n}^2 + \Delta_{sc}^2}$ , cf. Fig. 6c, thus yielding a spectral weight transfer as observed in Fig. (5). In this case we find  $\Delta_{SC} = \Delta_{Q_n=0} \approx 0.2t$  which is compatible with the separation of excitations in  $\sigma_{NL} - \sigma_{SC}$  for the transition #2.

---

[1] D. C. Mattis and J. Bardeen, Theory of the Anomalous Skin Effect in Normal and Superconducting Metals, Phys. Rev. **111**, 412 (1958).